

WASP-4 transit timing variation from a comprehensive set of 129 transits

R.V. Baluev^{1,2*}, E.N. Sokov^{1,2}, S. Hoyer³, C. Huitson⁴, José A.R.S. da Silva⁵,
P. Evans⁶, I.A. Sokova^{1,2}, C.R. Knight⁷, V.Sh. Shaidulin¹

¹*Saint Petersburg State University, Universitetskaya emb. 7–9, St Petersburg 199034, Russia*

²*Central Astronomical Observatory at Pulkovo of Russian Academy of Sciences, Pulkovskoje sh. 65/1, St Petersburg 196140, Russia*

³*Aix Marseille Univ, CNRS, CNES, LAM, Marseille, France*

⁴*CASA, University of Colorado, 389 UCB, Boulder, CO, 80309-0389, USA*

⁵*Department of Mathematical Sciences, University of South Africa, Private Bag X6, Florida 1709, South Africa*

⁶*El Sauce Observatory, Coquimbo Province, Chile*

⁷*Ngileah Observatory, 144 Kilkern Road, RD 1. Bulls 4894, New Zealand*

Accepted 2020 April 20. Received 2020 April 17; in original form 2020 March 10

ABSTRACT

We homogeneously reanalyse 124 transit light curves for the WASP-4 b hot Jupiter. This set involved new observations secured in 2019 and nearly all observations mentioned in the literature, including high-accuracy GEMINI/GMOS transmission spectroscopy of 2011–2014 and TESS observations of 2018. The analysis confirmed a nonlinear TTV trend with $P/|\dot{P}| \sim (17 - 30)$ Myr (1-sigma range), implying only half of the initial decay rate estimation. The trend significance is at least 3.4-sigma in the aggressively conservative treatment. Possible radial acceleration due to unseen companions is not revealed in Doppler data covering seven years 2007–2014, and radial acceleration of $-15 \text{ m s}^{-1} \text{ yr}^{-1}$ reported in a recent preprint by another team is not confirmed. If present, it is a very nonlinear RV variation. Assuming that the entire TTV is tidal in nature, the tidal quality factor $Q'_* \sim (4.5 - 8.5) \cdot 10^4$ does not reveal a convincing disagreement with available theory predictions.

Key words: planetary systems - techniques: photometric - stars: individual: WASP-4 - methods: data analysis

1 INTRODUCTION

The nonlinear trend in WASP-4 b transit timings was initially claimed by [Bouma et al. \(2019\)](#), based on new TESS observations acquired in 2018, and on ground-based observations published so far. According to their fit, its magnitude (curvature) corresponded to the period decay parameter $P/|\dot{P}| \sim 9.2$ Myr. One explanation of such a TTV trend is planet-star tidal interaction, causing either (i) planet spiraling on to the star, or (ii) tidal apsidal drift of a weakly eccentric planetary orbit. If the TTV trend and its tidal nature is confirmed, this target would be the second such example known, in addition to WASP-12.

However, in ([Baluev et al. 2019](#)) some doubts were raised concerning the reality of this TTV trend for WASP-4. In particular, it appeared that the trend is sensitive to just a few transit timings that may be affected by red noise or other systematic effects. Also, spurious TTV effects might

appear because of the heterogeneous nature of the timings. Since different transit observations were processed by different teams using different models and approaches, they may have different systematic errors. Even more importantly, timing uncertainties coming from different teams may have systematically different biases. Then some transit times with overstated accuracy may inadequately dominate over others, corrupting the results.

The TTV trend was neither confirmed nor retracted in ([Baluev et al. 2019](#)), but soon after that [Southworth et al. \(2019\)](#) presented a set of 22 additional WASP-4 transit observations apparently confirming its TTV trend at a high significance. However, they obtain a smaller TTV curvature than [Bouma et al. \(2019\)](#), while their analysis still did not take into account the issue of inhomogeneous data. Simultaneously, [Baluev et al. \(2019\)](#) did not reprocess two crucial sets of transit lightcurves from ([Hoyer et al. 2013](#); [Huitson et al. 2017](#)), because they were not published in table form. Without them, that homogeneous analysis of WASP-4 was not complete.

* E-mail: r.baluev@spbu.ru

Therefore, TTV studies currently available for WASP-4 are still disputable and incomplete in one concern or another. In this work our goal is to homogeneously analyse the comprehensive set of nearly all ground-based WASP-4 transit observations, including those from (Hoyer et al. 2013; Huitson et al. 2017; Southworth et al. 2019), and to verify the existence of the TTV trend.

In Sect. 2 we describe photometric data and their processing, while in Sect. 3 we present the main analysis results.

2 INPUT DATA AND THEIR PROCESSING

2.1 Transit photometry

We used most of the lightcurves from (Baluev et al. 2019). This includes (Wilson et al. 2008; Gillon et al. 2009; Sanchis-Ojeda et al. 2011; Nikolov et al. 2012; Petrucci et al. 2013), and amateur observations.

Recently, (Southworth et al. 2019) published a large amount of WASP-4 transit observations, including a replacement for (Southworth et al. 2009), as well as new light curves. Previously there were notices about clock errors affecting the Danish telescope used by Southworth et al. (2009), motivating Baluev et al. (2015, 2019) to remove those data from the TTV analysis. However, according to Southworth et al. (2019) that errors did not affect any WASP-4 observations. Therefore, in this work we use all these data without restriction.

We now use previously unpublished transit lightcurves from (Hoyer et al. 2013) and from (Huitson et al. 2017). The latter data are especially important, because they are of a very high accuracy, derived from the transmission spectroscopy at GEMINI. However, it was noticed in (Baluev et al. 2019) that transit times from (Huitson et al. 2017) might have understated uncertainties, possibly resulting in spurious or biased TTVs.

We also reanalysed 18 public TESS lightcurves available in the MAST (Mikulski archive). We removed all data that had nonzero quality indicator and cut out pieces ± 0.2 d around each transit (about 4 transit durations). The rest of the light curve was not used as it showed obvious hints of weak variability.

In 2019 we also obtained 6 new EXPANSION amateur observations of WASP-4, which are also included in this compilation. We therefore have now 124 transit lightcurves to be reprocessed homogeneously, compared to only 66 ones reprocessed by Baluev et al. (2019).

Finally, we used 5 old timings from (Gillon et al. 2009; Dragomir et al. 2011) without lightcurves, increasing the total transits number to $N = 129$. These timings are not so accurate, and their effect remains small.

As in (Baluev et al. 2019), we do not include the HST observations by Ranjan et al. (2014) because they were partly overexposed.

2.2 Lightcurves fitting and analysis

We used entirely the same processing pipeline as in (Baluev et al. 2019), simply adding new lightcurves at Stage 4 (full dataset) and Stage 5 (HQ dataset). The only major differ-

ence is that now we determine the HQ subset in a different more useful manner (detailed below).

Some important details of the algorithm are as follows. The lightcurves are fitted simultaneously against 3 planetary parameters common for all transits (the planet/star radii ratio, orbital impact parameter, transit duration), and individual transit timings. We also fit cubic trend in each lightcurve, and quadratic limb-darkening law on a band-per-band basis. The fitting is done using PLANETPACK3 software (Baluev 2018) through an advanced maximum-likelihood approach with regularized noise model described in (Baluev 2009; Baluev et al. 2015).

The resulting TTV data were fitted by a quadratic trend model with a curvature parameter $q = -\dot{P}/P$. This TTV model is linear with respect to its parameters, so even if q is small or zero, its uncertainty range remains meaningful and is nearly symmetric. The inverse $T_d = q^{-1}$ is perhaps a more intuitive quantity, the so-called period decay timescale, but it is not a linear parameter. If the uncertainty of σ_q appears comparable to q then confidence ranges for T_d are not symmetric.

This fitting was done via the maximum likelihood approach involving fittable noise (Baluev 2009), and using either multiplicative or so-called regularized noise model (Baluev 2015). That regularized noise model behaves mostly similar to the one with an additive “jitter” (Wright 2005), but mitigates some of its singular behaviour. For the full $N = 129$ dataset, we considered a total of 4 distinct models of the TTV noise, also depending on whether we treat this dataset as a whole or put the spotted transits (see below) into a separate subset with an independent noise model. See (Baluev et al. 2019) for further discussion of possible TTV noise models and their role.

2.3 Filtering out potentially corrupted lightcurves

WASP-4 demonstrates obvious spotting activity, and starspots appear as anomalies in the transit lightcurves (Sanchis-Ojeda et al. 2011). Such events disturb the shape of the lightcurve, building up additional noise in the derived transit times. According to Baluev et al. (2019), those errors may increase the TTV residuals r.m.s. by $\sim 30 - 100$ per cent, and may reach ~ 2 min (the case of HD 189733); see also (Barros et al. 2013; Oshagh et al. 2013). The putative WASP-4 TTV is below 1 min, so it can be significantly distorted by such errors.

This motivated us to apply some filter removing potentially unreliable transits, affected by spots. Notice that Southworth et al. (2019) undertook a similar work, but only for their own portion of data. Now we try to do this for the entire set of 124 lightcurves we have.

The first filter was targeted to remove transits affected by spots. For each lightcurve we computed the residuals r.m.s. $s_{\text{in/out}}$ for the in-transit and out-of-transit portions. If their ratio $\rho = s_{\text{in}}/s_{\text{out}}$ is large (compared to its uncertainty σ_ρ) then we may deal with a spot-transit anomaly. However, we avoided any formal thresholds on ρ , because this quantity is merely a rough indicator, e.g. it does not take into account any red noise. Instead, we adopted a simplified approach. We formed two ranged lists: one with increasing ρ and the other one with increasing significance of $\log \rho$, or $(\rho \log \rho)/\sigma_\rho$. After that, we extracted top quartiles from

Table 1. WASP-4: summary of transit data

Publication/Team	transits	unreliable
Sanchis-Ojeda et al. (2011)	6	4
Nikolov et al. (2012)	12	4
Petrucci et al. (2013)	6	2
Hoyer et al. (2013)	12	2
Huitson et al. (2017)	4	3
Southworth et al. (2019)	22	10
TRAPPIST	6	1
TESS-2018	18	3
others (mostly amateurs)	38	6
Total	124	35

the both lists. It appeared that both these top quartiles contained almost the same transits (with only a few exceptions). We finally constructed their intersection, forming the list of unreliable transits with only *significantly* large ρ . Finally, we also removed a few lightcurves that did not necessarily reveal clear spotting activity themselves, but were made at one of the same dates.

The second filter is a mixture of a periodogram analysis and jackknife. First, we noticed that the periodogram of TTV residuals (for our full dataset) demonstrated multiple spurious peaks that appear tall enough to pass formal significance threshold but visually looked like noise (similar to e.g. [Baluev et al. 2015](#)). Since this behaviour appears quite usual for WASP-4 and for a few other spotted targets, we suspected that the periodogram may simply reveal sensitivity to one or a few biased timings (corrupted by spots or other systematic errors). So to detect such bad points we subsequently removed one of them and recomputed the periodogram for each such reduced dataset. If the maximum periodogram peak changed too much after that, such a transit was identified as unreliable. The exact thresholds were subjective here, as we only wanted to identify clearly odd transits or those that offer abnormally high contribution into the results. We found just a few such odd lightcurves. After that, we also computed the formal significance of the quadratic TTV trend as q/σ_q and processed it in the similar way, identifying timings that contribute too remarkably. But this eventually did not highlight any new transits.

In the end of this procedure we had 89 HQ lightcurves out of the initial 124 ones. These two sets were passed through our primary pipeline independently. Thus, together with 5 third-party timings, we constructed two TTV datasets: the full one (129 points) and a homogeneous HQ one (89 points). They were obtained independently from each other, and are attached as online-only material (the format of the files is the same as in [Baluev et al. 2015](#)).

A summary of the filtered data is given in Table 1. As we can see, the most accurate observations reveal large fraction of potentially corrupted lightcurves, e.g. 3/4 of ([Huitson et al. 2017](#)), 2/3 of ([Sanchis-Ojeda et al. 2011](#)), and 1/2 of ([Southworth et al. 2019](#)), though only 1/6 of TESS-2018. On contrary, most amateur observations did not reveal detectable spots. Although expected, such behaviour is rather regretful, because the most accurate timings should likely have understated uncertainties and are not reliable because of that.

Notice that our filtering procedure was not supposed to be comprehensive, and several lightcurves in our HQ sample still demonstrate clear spot anomalies. For example, our method revealed 5 of 6 spots-affected lightcurves noticed by [Southworth et al. \(2019\)](#), additionally blacklisting 5 other their lightcurves. [Hoyer et al. \(2013\)](#) identified 4 possibly spotted transits, but none coinciding with our two. Simultaneously, they did not detect a spot in the transit of 2008/10/01 independently observed by [Southworth et al. \(2019\)](#). Given such inconsistencies, we assume it might be difficult to distinguish spot-transit anomalies from various systematic errors. Our goal here was to remove a predefined moderate fraction of empirically most unreliable lightcurves and to see how much the results would change then.

2.4 Doppler data and a self-consistent analysis

Any TTV trend may be an apparent effect of the unseen companion that causes variable light arrival delay (the Roemer effect, [Irwin 1952](#)). If the period of the companion is larger than the observation time span, it may induce a piece of a sinusoidal TTV variation following close to a parabola. However, such a companion would also reveal itself through radial acceleration (RA) of the host star. Therefore, Doppler measurement may help to discard such interpretation, or to put useful constraints.

We used here 99 radial velocity (RV) measurements available in ([Baluev et al. 2019](#)). This includes 49 HARPS measurements derived with HARPS-TERRA ([Anglada-Escudé & Butler 2012](#)), 45 CORALIE ones derived with a standard CORALIE reduction pipeline, and 5 Keck measurements from ([Knutson et al. 2014](#)).

The self-consistent fitting of the transit lightcurves and RV data was performed using the PLANETPACK software ([Baluev 2013, 2018](#)). The details are entirely the same as in ([Baluev et al. 2019](#)), in particular we adopted a fixed star mass of $0.930 M_{\odot}$ from ([Triaud et al. 2010](#)).

3 RESULTS

Our full TTV dataset, including all 129 transits, is shown in Fig. 1 of the online supplement, compared with some previous ([Bouma et al. 2019; Southworth et al. 2019](#)) and new fits of the TTV trend. Significant deviations are revealed between different trend models. According to [Southworth et al. \(2019\)](#), their estimate differs from [Bouma et al. \(2019\)](#) by about 2-sigma. This is rather large and possibly indicates some hidden systematic errors.

Our full TTV dataset suggests that the trend magnitude is now decreased even further, to about half of the value initially claimed ([Bouma et al. 2019](#)). It still depends on the noise model, but corresponds to $T_d \sim 15 - 20$ Myr, compared to 9.2 Myr following from ([Bouma et al. 2019](#)). The trend significance appears large, about 5–6 sigma, also model-dependent.

To estimate the trend significance we followed the same approach as in ([Baluev et al. 2019](#)). Given some probe value of q , we may compute the log likelihood-ratio statistic Z corresponding to the models with the best fitting \hat{q} and with the given q . The graph of $Z(q)$ should then have a nearly parabolic shape centered at \hat{q} . The value $Z(0)$ characterizes

the significance of the TTV trend itself (how much $q = 0$ agrees with the data), while horizontal Z -levels would determine confidence ranges for q , through intersections with $Z(q)$. As in (Baluev et al. 2019), we consider several significance levels from the χ^2 test, and the BIC ones.

Such plots are shown in Fig. 1. For the full TTV dataset $Z(0)$ becomes very high, above 5 sigma, but the shape of $Z(q)$ is sensitive to the noise model. Those model-variable changes correspond to shifts of about 1-sigma in terms of q . They might indicate that our full TTV dataset is still imperfect statistically. Some of its timings may be affected by systematic errors, e.g. caused by spot-transit events.

For the HQ subset, the trend significance is reduced to 3.4–3.8 sigma. The best quadratic fit for the TTV trend then becomes

$$\begin{aligned} \text{TTV}(n) &= T_0 + nP + q \frac{(nP)^2}{2}, \\ T_0 &= (2455937.080285 \pm 3.9 \cdot 10^{-5}) \text{ BJD}_{\text{TDB}}, \\ P &= (1.338231472 \pm 3.0 \cdot 10^{-8}) \text{ d}, \\ q &= (47 \pm 13) \text{ Gyr}^{-1} \end{aligned} \quad (1)$$

It is now almost model-invariable. This value of q corresponds to $T_d \simeq 21$ Myr and is close to the smallest value derived from the full TTV dataset. Therefore, this trend remains significant enough even in our aggressively conservative treatment, but its magnitude is smaller than previously claimed.

More importantly, $Z(q)$ became now considerably less model-sensitive. This might confirm that (i) we generally correctly removed the most unreliable lightcurves from our analysis, and (ii) the results derived from the HQ subset are statistically robust. Therefore, further removal of spotted lightcurves does not look very sensible. This would decrease the trend significance arbitrarily further, but simply because of reducing the number of available timings.

We can see that the full data (129 transits) already implied a reduction of q relatively to Southworth et al. (2019). This reduction was mainly because old data were reprocessed and old timings were corrected (not because of new data of 2019 that did not appear very accurate). However, after rejecting unreliable transits, q is reduced yet more. Therefore, these two effects join roughly 50/50.

In Table 2 we provide some parameters of our self-consistent fit of the RV and transit data. This fit relies on only 89 HQ transits reprocessed in this work. This fit allows us to estimate possible RV trend in the data (coefficient c_1). It is consistent with zero, and through the Roemer effect it would inspire the following TTV curvature:

$$q^{\text{RA}} = (2.6 \pm 3.9) \text{ Gyr}^{-1}. \quad (2)$$

As we can see, this value may only explain a minor portion of the observed q . The uncertainty in the tidal part of q remains almost unchanged as well.

4 DISCUSSION

The nonlinear TTV trend in WASP-4 reveals a confirmed high confidence, even in quite conservative treatment. Assuming the ‘separated regularized’ noise model, which is more adaptive, the TTV significance becomes somewhere

Table 2. WASP-4 self-consistent fit of transit and RV data.

num. of lightcurves N_{LC}	89 (HQ homogeneous)
num. of RVs N_{RV}	99
star mass $M_\star [M_\odot]$	0.93 (fixed)
star radius $R_\star [R_\odot]$	0.9019(47)
star density $\rho_\star [\rho_\odot]$	1.268(20)
rotation vel. $v \sin i [\text{m s}^{-1}]$	1970(260)
spin-orbit ang. $\lambda [^\circ]$	341(19)
rad. accel. $c_1 [\text{m s}^{-1} \text{ yr}^{-1}]$	−0.8(1.2)
planet mass $m [M_J]$	1.1974(68)
planet radius $r [R_J]$	1.3846(88)
orbital period ^{1,2} $P [\text{d}]$	1.338231602(56)
TTV trend ² $T_d [\text{Myr}]$	21.3(5.5)
mean longitude ¹ $l [^\circ]$	235.86(26)
inclination $i [^\circ]$	88.87(39)
eccentricity e	0.0053(38)
pericenter arg. $\omega [^\circ]$	247(28)
$e \cos \omega$	−0.0021(22)
$e \sin \omega$	−0.0049(41)

The fitting uncertainties are given in parenthesis after each estimation, in the units of the last two figures. The M_\star uncertainty was not included in the fit.

¹These parameters refer to $T_0 = 2455197.5$ (2015/01/01) in the BJD TDB system.

²The uncertainty in P and T_d should be scaled up by the TTV scatter $\sqrt{\chi^2_{\text{TTV}}} = 1.14$ to include the effect of remaining spots. Notice that P here is different from (1) because they refer to different epochs.

between 3.8-sigma (HQ data) and 4.8-sigma (full data), depending on how much spots perturb the derived timings.

Therefore, in addition to WASP-12 (Maciejewski et al. 2018) this target represents yet another such example. Still, the trend curvature for WASP-4 is estimated to be only half of what was claimed initially, and about 6 – 8 times more slow than for WASP-12. Based on formula (16) from (Bouma et al. 2019) and our fits, the modified quality factor becomes $Q'_\star \sim 60000$, with a 1-sigma range of 45000 – 85000. Given the large uncertainty, this is not too much small compared to theoretical predictions. For example, this agrees well with the estimation $Q'_\star \simeq (1.2^{+1.0}_{-0.5}) \cdot 10^5$ computed by Bouma et al. (2019) based on (Penev et al. 2018). In terms of a more Gaussian parameter $1/Q'_\star$, the displacement of these two estimations becomes just about 1.2-sigma.

Simultaneously, there is a wide range of predictions on Q'_\star in the literature, in particular those yielding a much larger value (Collier Cameron & Jardine 2018). It seems that both the WASP-12 and WASP-4 cases favour to the models implying rather small Q'_\star . WASP-4 transit observations should be continued in order to further refine its TTV.

In this work we considered only a tidal orbit decay model. The TTV interpretation through tidal apsidal drift is also possible (Patra et al. 2017), but it is unlikely to be robustly distinguished for WASP-4, given the small TTV magnitude.

While this Letter was in review, Bouma et al. (2020) reported a radial acceleration of WASP-4 of $-15 \text{ m s}^{-1} \text{ yr}^{-1}$, based on new Keck data. This would explain the observed TTV through the light arrival delay, but they did not use full CORALIE and HARPS data from Baluev et al. (2019). This full dataset appears strongly inconsistent with their value for c_1 , see Fig. 2 in the online-only supplement. The RV trend is only supported by a few recent Keck observations made after a long pause. This indicates that the RV variation they

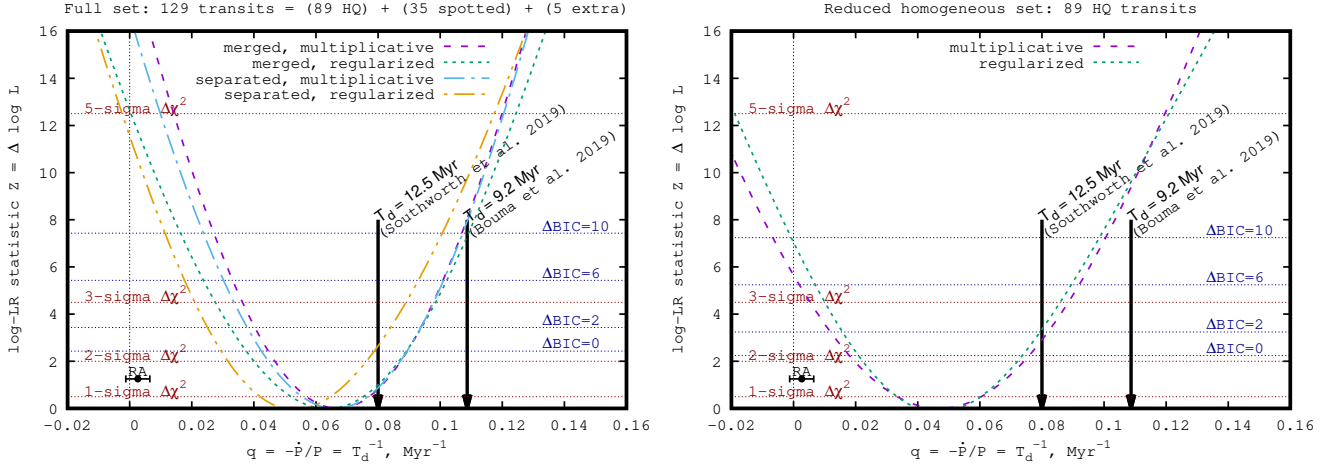


Figure 1. Logarithm of the likelihood ratio statistic for WASP-4, $Z(q)$, as a function of $q = -\dot{P}/P = T_d^{-1}$. Left panel is for the full dataset, right one is for the HQ one. Near-parabolic curves within each graph correspond to different models of the TTV noise, as labelled. In each graph a set of the significance threshold levels is shown, corresponding to the frequentist χ^2 test or to the BIC. The Roemer effect due to possible radial acceleration (RA) is shown as a horizontal errorbar. See text for more details.

captured looks like a severely nonlinear RV variation rather than constant radial acceleration. This makes their conclusions that RV variation can explain the TTV disputable. RV was nearly constant at least until 2014, while only recently accumulating observable bias. Such a nonlinear RV variation may induce a much smaller TTV than constant acceleration. We believe that results by Bouma et al. (2020) need to be reassessed in view of complete RV data, but this is a work for separate investigation.

ACKNOWLEDGEMENTS

Organization of the EXPANSION project (ENS, IAS), statistical analysis (RVB), and data collection (VSS), apart from the observations, were supported by Russian Science Foundation grant 19-72-10023. SH acknowledges CNES grant 837319 support for processing the observations. Authors would like to thank the TRAPPIST team for sharing their archival data, as well as the anonymous reviewer for their useful comments and suggestions.

REFERENCES

- Anglada-Escudé G., Butler R. P., 2012, *ApJS*, 200, 15
 Baluev R. V., 2009, *MNRAS*, 393, 969
 Baluev R. V., 2013, *Astron. & Comput.*, 2, 18
 Baluev R. V., 2015, *MNRAS*, 446, 1493
 Baluev R. V., 2018, *Astron. & Comput.*, 25, 221
 Baluev R. V., et al., 2015, *MNRAS*, 450, 3101
 Baluev R. V., et al., 2019, *MNRAS*, 490, 1294
 Barros S. C. C., Boué G., Gibson N. P., Pollacco D. L., Santerne A., Keenan F. P., Skillen I., Street R. A., 2013, *MNRAS*, 430, 3032
 Bouma L. G., et al., 2019, *AJ*, 157, 217
 Bouma L. G., Winn J. N., Howard A. W., Howell S. B., Isaacson H., Knutson H., Matson R. A., 2020, *ApJ, Lett*, arXiv:2004.00637
 Collier Cameron A., Jardine M., 2018, *MNRAS*, 476, 2542
 Dragomir D., et al., 2011, *AJ*, 142, 115

- Gillon M., et al., 2009, *A&A*, 496, 259
 Hoyer S., et al., 2013, *MNRAS*, 434, 46
 Huitson C. M., Désert J.-M., Bean J. L., Fortney J. J., Stevenson K. B., Bergmann M., 2017, *AJ*, 154, 95
 Irwin J. B., 1952, *ApJ*, 116, 211
 Knutson H. A., et al., 2014, *ApJ*, 785, 126
 Maciejewski G., et al., 2018, *Acta Astronomica*, 68, 371
 Nikolov N., Henning T., Koppenhoefer J., Lendl M., Masiejewski G., Greiner J., 2012, *A&A*, 539, 159
 Oshagh M., Santos N. C., Boisse I., Boué G., Montalto M., Dumusque X., Haghighipour N., 2013, *A&A*, 556, A19
 Patra K. C., Winn J. N., Holman M. J., Yu L., Deming D., Dai F., 2017, *AJ*, 154, 4
 Penev K., Bouma L. G., Winn J. N., Hartman J. D., 2018, *AJ*, 155, 165
 Petrucci R., Jofré E., Schwartz M., Cúneo V., Martínez C., Gómez M., Buccino A. P., Mauas P. J. D., 2013, *ApJ*, 779, L23
 Ranjan S., Charbonneau D., Désert J.-M., Madhusudhan N., Deming D., Wilkins A., Mandell A. M., 2014, *AJ*, 147, 161
 Sanchis-Ojeda R., Winn J. N., Holman M. J., Carter J. A., Osip D. J., Fuentez C. I., 2011, *ApJ*, 733, 127
 Southworth J., et al., 2009, *MNRAS*, 399, 287
 Southworth J., et al., 2019, *MNRAS*, 490, 4230
 Triaud A. H. M. J., et al., 2010, *A&A*, 524, A25
 Wilson D. M., et al., 2008, *ApJ*, 675, L113
 Wright J. T., 2005, *PASP*, 117, 657

This paper has been typeset from a \LaTeX file prepared by the author.